lacking essentially half of the exine is probably a unique feature of this family.

Apertures are openings or thin areas in the exine through which the pollen tube usually emerges at the time of germination. The evolution of apertures in pollen grains was one of the major advances of the seed plants and aperture type is one of the most important phylogenetic characters of pollen grains. Pteridophytes, in the strict sense, do not have apertures; however, they do have nonhomologous, thin areas called tetrad scars by which the spores often open. It was in gymnospermous plants that the first apertures evolved. Certain fossil gymnosperm pollen grains (for example, the pteridosperms) still have a tetrad scar on the proximal face (inward face of the meiotic tetrad) which is homologous to the tetrad scar of pteridophyte spores. The first true apertures, however, evolved at the distal pole (facing outward in the meiotic tetrad). One of the earliest concepts developed in comparative pollen morphology was that uniaperturate pollen always has the aperture at the distal pole (*7*). The validity of this hypothesis for pollen of the Annonaceae was first questioned by Bailey and Nast (*8*), and since then, the true nature of the annonaceous aperture has been open to some question (*3, 9*). From a study of more than 25 annonaceous genera in which tetrads or polyads occur, it is clear that in all except one of these the aperture is on the proximal face (Fig. 2A), not the distal pole as in all other known uniaperturate pollen. The genus *Pseudoxandra* R. E. Fries is of great palynological interest because one of its species (*P. coriacea* R. E. Fries) has a distal aperture, a second [*P. williamsii* (R. E. Fries) R. E. Fries] has a proximal one, and other species [*P. guianensis* (R. E. Fries) R. E. Fries, *P. leiophylla* (Diels) R. E. Fries, *P. polyphleba* (Diels) R. E. Fries] show transitional stages in the evolution of the distinctly annonaceous type of proximal aperture.

Most mature pollen grains are solitary (monads) within the thecal chambers of the stamen, but in a number of angiosperm families they are in dyads, tetrads, polyads, or pollinia, which consist of the entire pollen mass of a thecal chamber. Although there are approximately 50 families of angiosperms (41 dicot and 12 monocot families) in which all or some members have pollen grains in tetrads or dyads (*1*), polyads are rare. There are only three families in which polyads are well known—Leguminosae–Mimosoideae (*10*), Asclepiadaceae, and Orchidaceae. The latter two families are also the only angiosperm families with pollinia. The genus *Hippocratea* L. (Hippocrateaceae) also has polyads (*11*), as have genera in the Gentianaceae (*12*). To this rather restricted list may be added the seven annonaceous genera of the *Cymbopetalum* tribe as well as certain species of the more distantly related genus *Xylopia* L. [*X. brasiliensis* Spreng., *X. ferruginea* (Hk.f. & Th.) Hk.f. & Th., *X. micans* R. E. Fries, *X. africana* (Benth.) Oliv.]. Until now, the occurrence of polyads in the Annonaceae was not recognized generally (*13*). The polyads in this family are easily disrupted by acetolysis, and clearing of stamens with careful dissection is often necessary to preserve them. From such studies the following types of polyads have been found: octads in *Cymbopetalum* (Fig. 2B), *Cardiopetalum* Schlecht., *Froesiodendron* R. E. Fries, *Trigynaea* Schlecht., and *Disepalum* Hk.f.; polyads of 16 grains in *Hornschuchia* Nees; and variable polyads of 16, 18, 20, 24, or more grains in *Porcelia* Ruiz & Pav. (Fig. 2C) (*14*). It is interesting to note that *Xylopia* and all the genera of the *Cymbopetalum* tribe except *Disepalum* have transversely locellate anthers at maturity, with each polyad in a separate compartment within the stamen (Fig. 2C).

JAMES W. WALKER

Department of Botany,
University of Massachusetts,
Amherst 01002

References and Notes

1. J. W. Walker, *Contrib. Gray Herb. Harvard*, in press.
2. A. pollen unit is the grouping in which pollen is found at maturity within the stamen, that is, whether in monads (solitary grains), tetrads, polyads, and so forth.
3. G. Erdtman, *Pollen Morphology and Plant Taxonomy. Angiosperms* (Hafner, New York, 1966).
4. G. Erdtman, *Handbook of Palynology* (Hafner, New York, 1969), p. 34.
5. P. Echlin, *Sci. Amer.* **218** (4), 81 (1968).
6. K. Faegri and J. Iversen, *Textbook of Pollen Analysis* (Hafner, New York, ed. 2, 1964), p. 15.
7. R. P. Wodehouse, *Pollen Grains* (Hafner, New York, 1965), pp. 322–331.
8. I. W. Bailey and C. G. Nast, *J. Arnold Arboretum* **24**, 340 (1943).
9. J. E. Canright, *Grama Palynol.* **4**, 64 (1963); L. A. Kuprianova, *Rev. Palaeobot. Palynol.* **3**, 73 (1967).
10. P. Sorsa, *Ann. Bot. Fenn.* **6**, 1 (1969).
11. A. S. Bartlett, *Palynological Studies of the Gatun Basin, Panama*, thesis, Harvard University (1967).
12. S. Nilsson, *Svensk. Bot. Tidsk.* **64**, 1 (1970).
13. F. A. G. Miquel, in Martius' *Flora Brasiliensis* (vol. 7, pp. 18–19 and pl. 7, figure 12), evidently was the first to picture an annonaceous polyad in 1856 as part of his plate of the genus *Hornschuchia*; it appears that no one has looked since for the occurrence of polyads within the family.
14. Although material is lacking, the floral description of *Bocagea* St. Hil. suggests its placement within the *Cymbopetalum* tribe also.
15. Pollen photographs are vouchered by the following specimens: *Cymbopetalum odoratissimum* Barb. Rodr., B. A. Krukoff 4646 (NY), P-550 (author's palynological accession number); *Asteranthe asterias* (S. Moore) Engl. & Diels, Faulkner 3683 (K), P-773; *Cymbopetalum gracile* R. E. Fries, G. B. Hinton et al. 10257 (US), P-637; *Porcelia steinbachii* (Diels) R. E. Fries, B. A. Krukoff 5676 (NY), P-577. A set of the author's permanent pollen slides is on deposit in the Paleobotanical Collections of the Botanical Museum of Harvard University.

16. I thank the directors and curators of the following herbaria for use of palynological material from their collections: New York Botanical Garden; U.S. National Herbarium, Washington, D.C.; and the Royal Botanic Gardens, Kew, Great Britain. I am indebted to Jeolco, Inc., Medford, Massachusetts, for use of their JSM-2 scanning electron microscope. I gratefully acknowledge discussions with Dr. James A. Doyle.

7 December 1970; revised 11 March 1971 ■

Quadratic Elongation: A Quantitative Measure of Distortion in Coordination Polyhedra

Abstract. *Quadratic elongation and the variance of bond angles are linearly correlated for distorted octahedral and tetrahedral coordination complexes, both of which show variations in bond length and bond angle. The quadratic elongation is dimensionless, giving a quantitative measure of polyhedral distortion which is independent of the effective size of the polyhedron.*

Various criteria have been proposed to describe the distortions of coordination polyhedra from their holosymmetric geometries. In coordination chemistry octahedral complexes are often found to be distorted from O_h symmetry. There are two limiting types of distortion. Extension or compression along an S_6 axis of the octahedron is called trigonal distortion. The result is a trigonal antiprism with D_{3d} symmetry whose angles deviate from 90° but whose metal-anion distances remain equal in length. Extension or compression along a C_4 axis is called tetragonal distortion. The result is a tetragonal bipyramid with D_{4h} symmetry whose metal-anion distances change but whose angles remain equal to 90°. In many cases, particularly in minerals, distortions from O_h symmetry are more complex, involving changes in both octahedral bond lengths and angles. For example, distortions of the $M(1)O_6$ and $M(2)O_6$ octahedra in the olivines, $(Mg,Fe)_2SiO_4$, have been described in terms of differences in bond lengths (*1*), local symmetry (*2*), and bond angle strains (*3*). But none of these descriptions is satisfactorily quantitative.

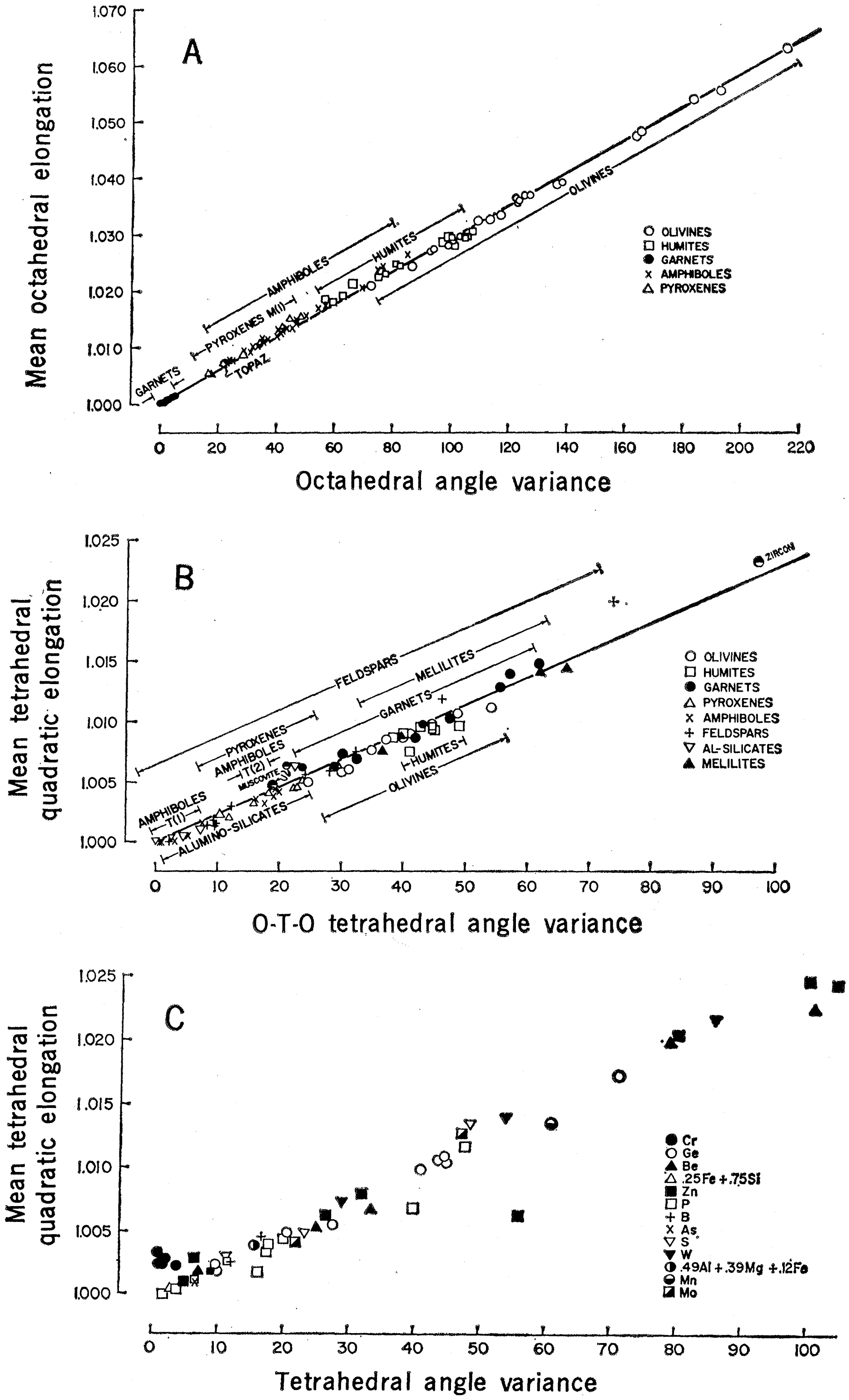

Fig. 1. (A) Mean quadratic elongation for octahedra in a variety of mineral groups plotted against octahedral angle variance. (B) Mean quadratic elongation for tetrahedra in a variety of silicates and aluminosilicates plotted against tetrahedral angle variance. (C) Plot similar to Fig. 1B for tetrahedra containing cations other than Si or Al. The fractional part of the quadratic elongation parameter is approximately equal to twice the percentage deviation of the polyhedron from its holosymmetric configuration. For example, $\lambda = 1 + 2\Delta l/l_0$. If $\lambda = 1.06$, then $\Delta l/l_0 = 0.03$.

Recently we have found that the variance of the octahedral angles

$$\sigma_{\theta(\mathrm{oct})}^2 = \sum_{i=1}^{12} (\theta_i - 90°)^2/11$$

is a convenient and realistic measure of distortion for those octahedra that show variations in both bond length and bond angle. This is illustrated in Fig. 1A where σ_θ^2 is seen to vary linearly with the mean octahedral quadratic elongation. The quadratic elongation is a convenient measure of distortion often used in the analysis of finite homogeneous strain (*4*). It is defined as

$$\lambda = \left(\frac{l_i}{l_0}\right)^2 = \left(\frac{l_0 + \Delta l}{l_0}\right)^2 \approx 1 + \frac{2\Delta l}{l_0}$$

where l_0 is the length of a line in the unstrained state, and l_i is the length of the line in the strained state. On the basis of this definition we have calculated mean octahedral quadratic elongation parameters (Fig. 1A)

$$\langle\lambda_{\mathrm{oct}}\rangle = \sum_{i=1}^{6} (l_i/l_0)^2/6$$

where l_0 is the center-to-vertex distance for an octahedron with O_h symmetry whose volume is equal to that of the strained or distorted octahedron with bond lengths l_i.

Similar variances and elongation parameters can be calculated for any defined coordination polyhedron. For tetrahedral complexes and coordination polyhedra

$$\sigma_{\theta(\mathrm{tet})}^2 = \sum_{i=1}^{6} (\theta_i - 109.47°)^2/5$$

and

$$\langle\lambda_{\mathrm{tet}}\rangle = \sum_{i=1}^{4} (l_i/l_0)^2/4$$

Figure 1, A and B, shows that for a large number of rock-forming minerals strong linear correlations exist between $\langle\lambda_{\mathrm{oct}}\rangle$ and $\sigma_{\theta(\mathrm{oct})}^2$ (correlation coefficient $\hat{R}_1 = 0.99$) and between $\langle\lambda_{\mathrm{tet}}\rangle$ and $\sigma_{\theta(\mathrm{tet})}^2$ ($\hat{R}_1 = 0.91$). Since λ is dimensionless, it is not surprising that both large and small cation-containing octahedra (Fig. 1A) and tetrahedra (Fig. 1, B and C) fall on the same line when plotted against $\sigma_{\theta(\mathrm{oct})}^2$ and $\sigma_{\theta(\mathrm{tet})}^2$, respectively. The tetrahedra plotted in

Fig. 1B contain only Si or Al, or both, whereas those in Fig. 1C contain Be, B, Mg, P, S, Cr, Mn, Fe, Zn, Ge, As, Mo, and W. These figures suggest that angular variance and quadratic elongation give similar quantitative measures of polyhedral distortion for many compounds. However, in certain cases where pronounced Jahn-Teller distortions are apparent and where the metal cation is coordinated both by anions and by molecules such as H_2O, the angular variance may not be a valid measure of polyhedral distortion. For example, in dioptase, $CuSiO_3 \cdot H_2O$, Cu is coordinated by four oxygen atoms in a square planar array at 1.95 to 1.98 Å and by two H_2O molecules at 2.50 and 2.65 Å, forming a tetragonally distorted octahedron (*5*). The angular variance of this octahedron is 85.7 from which a quadratic elongation of 1.025 is predicted according to Fig. 1A, whereas the calculated value is 1.061. This means that angular variance, although easily computed, cannot always be relied on to give as true a measure of polyhedral distortion as quadratic elongation. Neither bond length range nor bond length variance shows meaningful correlation with angular variance or quadratic elongation.

Using the range of bond angle strains as a measure of octahedral distortion in olivines, Brown (*3*) demonstrated that octahedra containing smaller divalent cations (Ni^{2+}, Mg^{2+}, Fe^{2+}) are less distorted than those containing Ca^{2+}. This is substantiated in Fig. 2, A and B, which shows that distortions of the M(1) and M(2) octahedra are linearly dependent on the effective size of the octahedral cation. Using the range of bond angle strains or the range of bond lengths, one would conclude that the

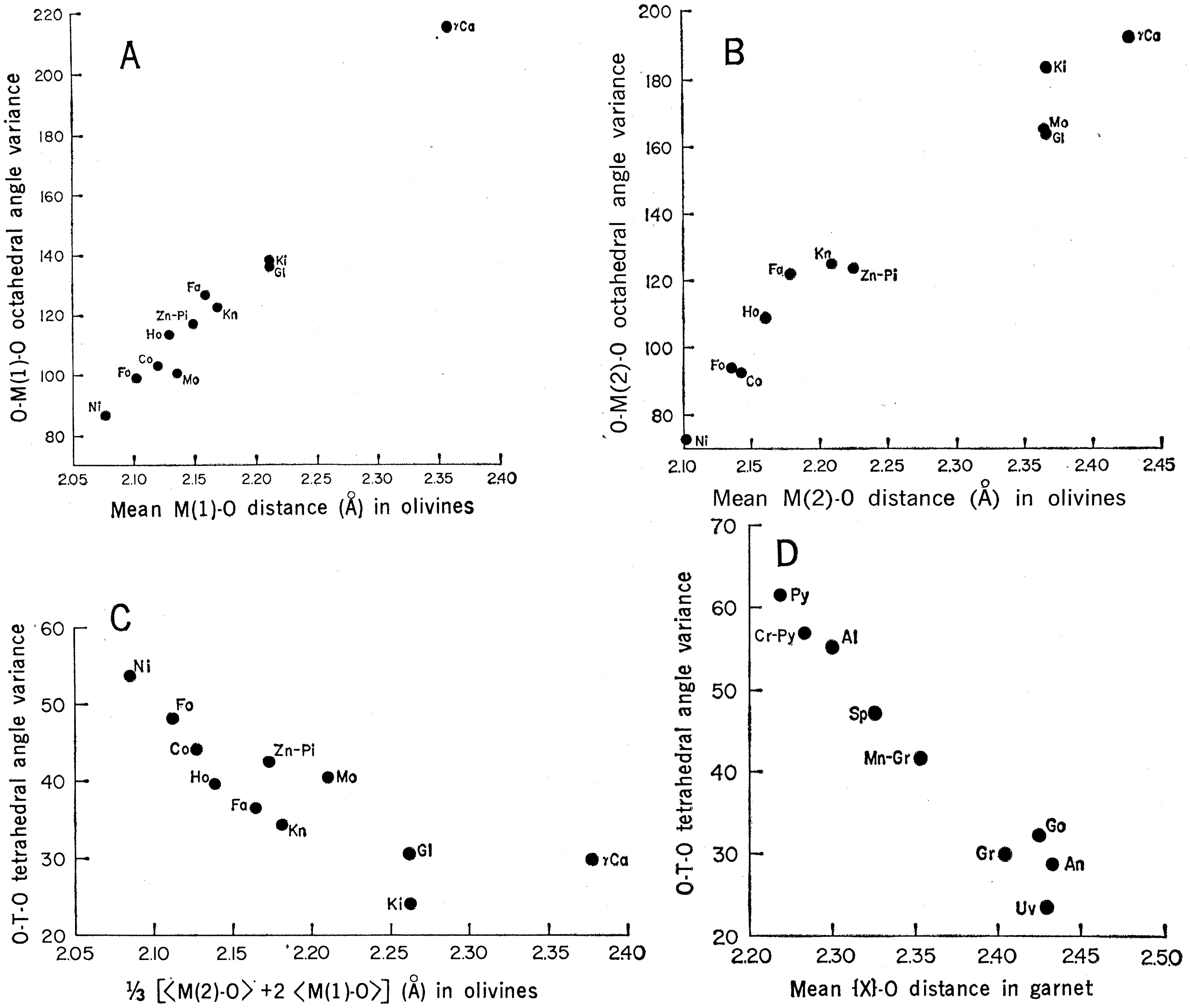

Fig. 2. (A) The O–M(1)–O octahedral angle variance in olivines as a function of the effective size of the M(1) cation, represented here by the mean M(1)–O distance. Ni, synthetic Ni_2SiO_4; Fo, forsterite; Co, synthetic Co_2SiO_4; Ho, hortonolite; Fa, fayalite; Zn-Pi, zinc picrotephroite; Kn, knebelite; Mo, monticellite; Ki, kirschsteinite; Gl, glaucochroite; γCa, synthetic γ-Ca_2SiO_4. (B) The O—M(2)–O octahedral angle variance in olivines as a function of the effective size of the M(2) cation, represented by the mean M(2)–O distance. (C) The O–T–O tetrahedral angle variance in olivines as a function of the mean size of the octahedra which share edges with the tetrahedron. (D) The O–T–O tetrahedral angle variance in garnets as a function of the mean {X}–O distance in edge-sharing dodecahedra. Py, pyrope; Cr-Py, chromium pyrope; Al, almandine; Sp, spessartine; Mn-Gr, manganese grossular; Gr, grossular; Uv, uvarovite; Go, goldmanite; An, andradite.

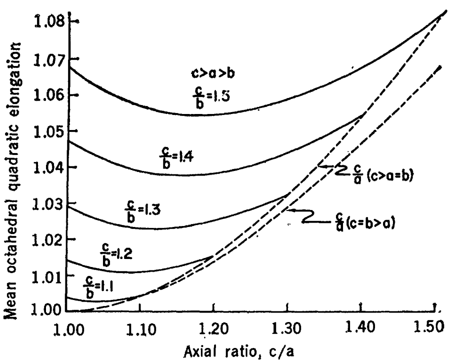

Fig. 3. Mean octahedral quadratic elongation as a function of axial ratios for octahedra with $a \neq b \neq c$; dashed curves are for tetragonally distorted octahedra.

larger M(2) octahedra are more distorted than the smaller M(1) octahedra. However, both the quadratic elongation and the angular variance parameters indicate that M(1) is slightly more distorted than M(2) for disordered olivines and for those containing only one type of octahedral cation.

Figure 2C shows that distortion of the SiO_4 tetrahedron in olivine is related to the effective size of the cations in the octahedra with which it shares edges. Likewise, distortion of the SiO_4 tetrahedron in garnet (Fig. 2D) is dependent on the effective size of the {X} cation in the edge-shared dodecahedra (*6*). In both structure types the tetrahedra become more regular as the cations in the edge-shared polyhedra become larger. For those distorted polyhedra whose bond angles are ideal, for example, an octahedron with D_{2h} or D_{4h} symmetry, the angular variance cannot be used as a measure of distortion. In this case, the quadratic elongation can be calculated with ease, since $l_0 = (a \cdot b \cdot c)^{1/3}$, where *a*, *b*, and *c* are the three center-to-vertex distances in the octahedron. Graphical solutions can be obtained with the use of Fig. 3 in the following manner. For octahedra with D_{2h} symmetry, one would (i) order the metal-anion distances $c>a>b$, (i) find the value of the ratio c/a along the abscissa, and (iii) plot the ratio c/b among the family of solid curves. For tetragonally distorted octahedra, one would (i) compute the ratio c/a and (ii) use either the upper dashed curve if *c* is the unique axis ($c > a = b$) or the lower dashed curve if *a* is unique ($c = b > a$).

If the mean quadratic elongation is used as a quantitative measure of polyhedral distortion, it now should be possible to separate by regression analysis the roles played by distortion and by size in determining the distribution of cations among coexisting phases as well as the polyhedral site preferences within a single phase.

KEITH ROBINSON*
G. V. GIBBS
P. H. RIBBE

Department of Geological Sciences,
Virginia Polytechnic Institute and
State University, Blacksburg 24061

References and Notes

1. S. Ghose, in *Handbook of Geochemistry*, K. H. Wedepohl, Ed. (Springer-Verlag, Berlin, 1969), vol. 2, part 1, p. 26-A-7.
2. R. G. Burns, *Mineralogical Applications of Crystal Field Theory* (Cambridge Univ. Press, Cambridge, 1970), pp. 119–127; *Amer. Mineral.* 55, 1608 (1970).
3. G. E. Brown, thesis, Virginia Polytechnic Institute (1970).
4. J. C. Jaeger, *Elasticity, Fracture and Flow* (Methuen, London, ed. 2, 1962), p. 34.
5. M. M. Hamil and P. H. Ribbe, *Geol. Soc. Amer. Southeastern Sect. Meetings* (1971).
6. G. A. Novak and G. V. Gibbs, *Amer. Mineral.*, in press.

7. We thank Dr. M. Hamil for bringing the concept of quadratic elongation to our attention and Dr. S. J. Louisnathan for critically reading the manuscript. Study supported by NSF grant GA-12702.

* Present address: Exploration Research, U.S. Geological Survey, Denver, Colorado 80225.

21 December 1970 ■

Maintenance of Resting Potential in Anoxic Guinea Pig Ventricular Muscle: Electrogenic Sodium Pumping

Abstract. *Anoxic ventricular muscle maintained a normal resting potential despite a large loss of potassium. The resting potential was separated into two components: one that depended on the potassium distribution, and one that depended on the activity of an electrogenic sodium pump.*

The ionic hypothesis states that the resting potential of excitable cells results from the distribution of ions across a selectively permeable cell membrane (*1*). The potassium concentration gradient has been considered responsible for the resting potential of muscle cells. Slight measured deviations of the membrane from the behavior of a simple potassium electrode have been accounted for by permeability of the membrane to other ions such as sodium and chloride (*2*). If the resting potential is dependent on potassium distribution, and if both intracellular and extracellular potassium concentrations are known, then the value of the resting potential may be predicted by the Nernst equation

$$E_k = \frac{RT}{F} \ln \frac{[K]_o}{[K]_i}$$

where E_k is the potassium equilibrium potential, R is the gas constant, T is the absolute temperature, F is the Faraday constant, $[K]_o$ is the extracellular potassium concentration, and $[K]_i$ is the intracellular potassium concentration. On the other hand, if the sodium gradient also contributes to the resting potential (*3*), the resting potential observed will be lower than that predicted by E_k, particularly at external potassium concentrations in the physiological range (*4*).

Earlier studies (*5*) have shown that guinea pig papillary muscles incubated under anoxic conditions for up to 12 hours have a normal resting potential as judged from the amplitude of the action potential. On the other hand, anoxic muscles have been shown to lose much of their potassium (*6*). Analysis of ^{42}K efflux data indicated the possibility of cell compartmentalization of potassium (*6*), since a rapidly exchanging compartment contained five times more the amount of potassium than that attributable to the extracellular (inulin) space. It was tentatively pro-

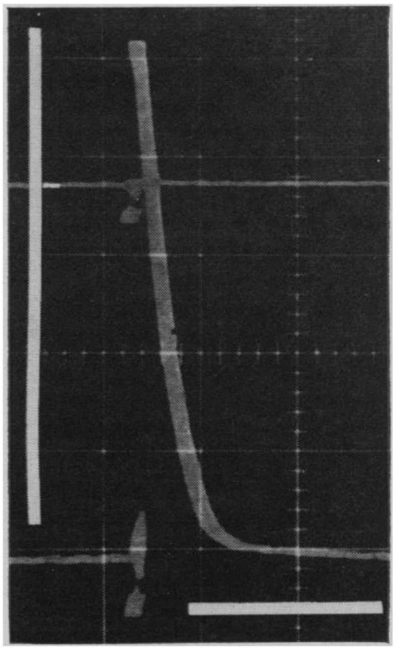

Fig. 1. Action potential of a guinea pig papillary muscle after 8 hours of anoxic incubation in 5 m*M* glucose medium. Voltage calibration is 100 mv and time calibration is 100 msec. Horizontal line across voltage indicates zero potential.